Clays and Clay Minerals, Vol. 41, No. 5, 613–623, 1993.

KAOLINITE PARTICLE SIZES IN THE <2 μM RANGE USING LASER SCATTERING

IAN D. R. MACKINNON, PHILIPPA J. R. UWINS, ANYA YAGO, AND DAVID PAGE

Centre for Microscopy and Microanalysis, The University of Queensland
St. Lucia QLD 4072 Australia

Abstract—The Clay Minerals Society Source Clay kaolinites, Georgia KGa-1 and KGa-2, have been subjected to particle size determinations by 1) conventional sedimentation methods, 2) electron microscopy and image analysis, and 3) laser scattering using improved algorithms for the interaction of light with small particles. Particle shape, size distribution, and crystallinity vary considerably for each kaolinite. Replicate analyses of separated size fractions showed that in the <2 μm range, the sedimentation/centrifugation method of Tanner and Jackson (1947) is reproducible for different kaolinite types and that the calculated size ranges are in reasonable agreement with the size bins estimated from laser scattering. Particle sizes determined by laser scattering must be calculated using Mie theory when the dominant particle size is less than ~5 μm. Based on this study of two well-known and structurally different kaolinites, laser scattering, with improved data reduction algorithms that include Mie theory, should be considered an internally consistent and rapid technique for clay particle sizing.

Key Words—Kaolinite, Laser scattering, Particle size.

INTRODUCTION

Detailed studies of kaolins from a range of different localities show that these clays occur in a wide variety of forms of varying crystalline perfection and show wide ranges of particle size distributions. Kaolins from the Georgia region alone demonstrate a range of crystal perfection from "well ordered" to "poorly ordered," and contain variable proportions of crystalline and non-crystalline material (e.g., Hinckley, 1963; Fripiat and van Olphen, 1979). The structural order or disorder of kaolinite grains has been studied, usually by powder X-ray diffraction (XRD) methods, in order to correlate such data with geological environment, mechanical processing (such as grinding or transport), or industrial utility (Murray and Lyons, 1956; Brindley *et al.*, 1986). In addition, studies that assess the variation of a kaolinite property with particle size have noted widely varying correlations between, for example, particle size and "crystallinity index" for a given kaolinite sample (Olivier and Sennett, 1973; Brindley *et al.*, 1986; Tettenhorst and Corbato, 1986; Lombardi *et al.*, 1987). Some of this particle size variation observed in natural samples may be due to inappropriate use of sizing techniques for a particular size range (e.g., McCave *et al.*, 1986), poor reproducibility of the sizing technique; or, alternatively, this may be due to natural variations in kaolin size distributions with a specific property. For some clays, the <2 μm size range is an important fraction that may determine the nature of bulk physical properties. Indeed, as shown by Lombardi *et al.* (1987) marked differences in structural and compositional properties can be obtained between size fractions of the same kaolin.

In most, if not all, cases, particle size fractions are determined by the gravitational settling method outlined by Tanner and Jackson (1947) or variations on this approach. This method is practical for particle sizes greater than about 2 μm equivalent spherical diameter. Thus, some size distribution studies have included sample splits into size fractions greater than 2 μm, with all smaller particles classified into the <2 μm fraction. For <2 μm particles, separation into smaller-sized fractions can be effected by centrifugation using the nomograms and algorithms developed by Tanner and Jackson (1947). As noted by Lombardi *et al.* (1987) and others, the size range of these separates bears only a nominal relationship to the actual sizes of the separated particles due to the non-spherical shape of kaolinite particles and their subsequent settling behaviour in an aqueous solution. In this study, no attempt is made to correct for the particular shape of individual clay particles or to average shape effects in the calculation of size distributions. Corrections for particle shape are possible with the laser scattering process described below (Brown and Felton, 1985), but are outside the scope of this study. Furthermore, size distribution methods commonly used for clays do not correct for shape in any rigorous fashion. Hence, all methods commonly used will inherently contain a systematic error related to the presumed average shape of clay particles.

With the advent of laser-based particle sizing techniques, a rapid basis for the determination of size distributions from low concentrations or small quantities of sample emerged, particularly for spherical particles of diameter >10 μm (Cornillault, 1972). A comparison of laser scattering techniques with conventional sieving-pipette methods showed that, for ten standard soil samples, there was good agreement between the two methods for size ranges from about 16 μm to 62 μm (Cooper *et al.*, 1984). However, data obtained via laser

Copyright © 1993, The Clay Minerals Society

https://doi.org/10.1346/CCMN.1993.0410512 Published online by Cambridge University Press

scattering for size ranges <16 μm and, in particular, for the 1.9 μm to 3.0 μm size range showed the poorest agreement with the conventional sedimentation method. Another evaluation of a laser scattering particle sizer from a competing manufacturer by McCave *et al.* (1986) showed similarly poor results for small-sized particles. Results for clay-sized particles were particularly disappointing, being neither accurate nor precise (McCave *et al.*, 1986).

In both these cases, the Fraunhofer diffraction theory was used to model the forward scattering of light. Bayvel and Jones (1981) noted that particles smaller than between 2 μm to 7 μm should not be sized using Fraunhofer diffraction models (depending on whether the particles are transparent or opaque) as errors in excess of 20% will occur. In general, the reason for these errors in this size range is that the wavelength of the incident light must be significantly smaller than the size of the particle to be measured. For He-Ne lasers (the most commonly used), the wavelength is $\sim$0.6 μm and thus, particles to be measured must be significantly larger than 1 μm (Miller and Lines, 1988). However, other studies have shown that the laser scattering method, when combined with an appropriate data reduction algorithm such as the Mie model for light scattering (Mie, 1908), provides good estimates of particle size distributions for sizes much closer to the wavelength of incident light (e.g., Dodge, 1987; de Boer *et al.*, 1987).

In this paper, we discuss the application of improved laser scattering instrumentation to particle size analyses of kaolinite clays that show various crystallographic and morphological properties. A comparison of particle size distributions calculated using Fraunhofer and Mie scattering theories is also undertaken for selected kaolinite samples to demonstrate the variations in capability of the respective algorithms used to reduce laser scattering data. In addition, we report on a study of kaolinite size fractions separated by the method of Tanner and Jackson (1947). This comparison of measured particle size fractions in the <2 μm diameter range provides an assessment of the effectiveness of the size fractionation by centrifugation process.

EXPERIMENTAL MATERIALS AND METHODS

Materials

Kaolinite samples from the CMS Source Clays from Georgia, KGa-1 and KGa-2 (Fripiat and van Olphen, 1979), as well as a sample from an Australian deposit, an actively mined site at Weipa, were chosen for this study. The Weipa sample is included in this study to illustrate specific difficulties associated with size fractionation of clays. The kaolinites, Georgia KGa-1 and KGa-2, are from Cretaceous and Tertiary brackish to marine environments with waters of similar isotopic composition (Hassanipak and Eslinger, 1985). The Georgia samples represent kaolinite crystallographic properties of widely varying type, including Hinckley indices for "well-crystallized" and "poorly-crystallized" clays (Hinckley, 1963) or, alternatively, both single phased and biphased defect structure types (Plancon and Zacherie, 1990). In general, differences in the degree of disorder appear related to differences in the geological environments of kaolinite accumulation (Brindley *et al.*, 1986).

Particle size fractionation

Well-dispersed kaolinite samples were prepared by adding 100 ml of ultra-pure water to 5g of kaolinite. This solution was placed in an ultrasonic tank for 15 min. Three ml of 10% Calgon solution were added to this slurry as an antiflocculant. The aqueous suspension was then separated into six size fractions by repeated centrifugation following the method outlined by Tanner and Jackson (1947). Each size fraction was dried in an oven at 120°C and subsequently weighed on a Mettler balance to determine the weight percentage abundance of each separate with respect to the bulk sample. For most samples, the smallest size fraction (i.e., <0.3 μm, or fraction "F") proved very difficult to characterize by the laser scattering technique due to coagulation of particles during analysis and, thus, data are not reported for this fraction. For samples KGa-1 and KGa-2, replicate size fractionations were performed in order to estimate the level of reliability of the sedimentation process.

Characterization

Imaging methods. Transmission electron microscopy (TEM) was performed on samples dispersed on carbon films using the following instruments: a JEOL 4000FX operating at 400 kV equipped with a Link Ge energy dispersive spectrometer (EDS) and Moran Scientific Analyser, a Philips 400T operating at 120 kV, and a Hitachi H-800 operating at 200 kV. Over this range of operating voltages, variations in electron beam damage rates were observed for some samples. In specific cases, this beam damage was minimized by the use of a Gatan LN_2 double tilt holder. Scanning electron microscopy (SEM) was undertaken with two instruments: a JEOL 6400F and a JEOL 890F both equipped with field emission guns. In general, both SEMs were operated at low accelerating voltages (i.e., <5 kV) as the majority of samples were examined without a conductive coating. The JEOL 6400F was equipped with a Link ultra-thin window Si(Li)EDS and Moran Scientific Analyser. Image analysis for particle sizing utilized a Wild Leitz MD-30+ image analysis system that included a video camera with 512 $\times$ 512 pixel size for capture of optical or electron-optical images. Standard image processing software was used to reduce raw data to compiled size distributions.

Estimates of particle size distributions within each

https://doi.org/10.1346/CCMN.1993.0410512 Published online by Cambridge University Press

size fractionated sample were obtained 1) by weight of kaolinite and 2) by laser scattering of dispersed samples. These two approaches are not directly comparable, as they measure quite different parameters of each sample (e.g., mass and light scattering), but they provide an approximate guide to the interpretations provided in the discussion section. Individual particle sizes of a standard spherical sample with nominal monomodal size distribution have been obtained by calibrated measurements from SEM micrographs. In general, over 1500 measurements have been made in order to estimate the size distribution of this standard material.

Diffraction methods. Particle size distributions may be measured over the range 0.1–600 μm using laser scattering in a flow-through cell with a Malvern Mastersizer E. For experiments reported here, only the size range from 0.1–80 μm was examined using the 45 mm lens of the Malvern Mastersizer E. During analysis, samples were constantly stirred in a 25 ml water suspension containing 3 ml of 10% Calgon solution. In the Malvern Mastersizer E used, the beam diameter is 13 mm, and the path length in the sample cell is 14.3 mm for all experiments reported. For all sizings of kaolinites using laser diffraction, the refractive index for kaolinite was used in the data reduction algorithm. All scattering data, except the Fraunhofer models shown in Figures 4 and 6, were reduced to size distributions using Mie theory. Techniques for size determination via laser scattering are well established and are documented in the particle characterization literature (Allen, 1981; Miller and Lines, 1988). Replicate analyses of the same sample, as well as replicate analyses of sample fractions (using the method of Tanner and Jackson, 1947), were analyzed by the Malvern Mastersizer E. For replicate analyses, estimated standard deviations for each mean value are calculated by standard statistical techniques and are shown in parentheses to the last significant figure of each value (i.e., 2.47(3) means 2.47 ± 0.03).

RESULTS

Imaging method

Measurement of kaolinite grain sizes from SEM and TEM micrographs shows that the centrifuge/sedimentation procedure of Tanner and Jackson (1947) generally produced well-defined, unimodal size fractions. Typical SEM micrographs of three different size fractions ("A," "C" and "E," respectively) for the Weipa sample are shown in Figure 1. SEM micrographs of the large size fraction of KGa-1 show similar morphologies to the Georgia kaolinite presented by Lombardi *et al.* (1987). The larger-sized grains in KGa-2 are less defined with embayed edges.

For the smaller particles, measured particle sizes within individual fractions varied by less than 0.3 μm

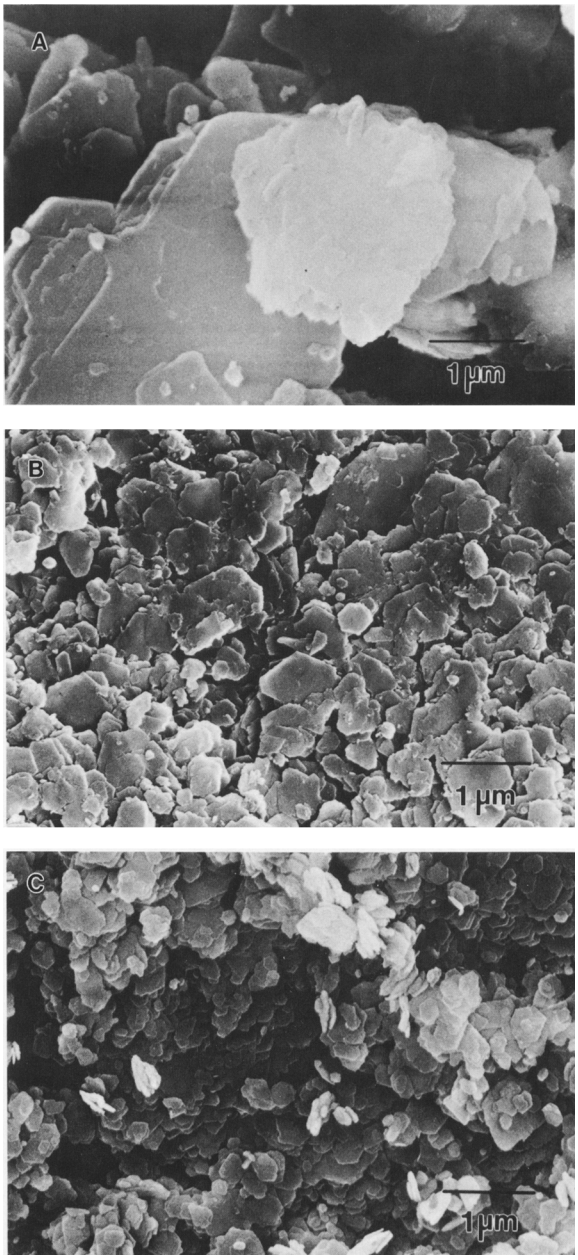


Figure 1. Scanning electron micrographs of size separated fractions of the Weipa sample: A) fraction A, >2.0 μm; B) fraction C, between 0.5 μm and 0.6 μm; and C) fraction E, between 0.3 μm and 0.4 μm. Each size fraction appears uniform in distribution and progressively smaller in size.

using measurements from electron micrographs. However, in the largest size fraction, "A," the variation in grain size was high. Micrographs from a sample of Weipa kaolinite, which was subjected to the same type of size fractionation and preparation, illustrate the reason for this variation in size for the largest fraction. Figure 2A shows a TEM micrograph of the bulk sample, while Figure 2B shows the large-sized fraction

https://doi.org/10.1346/CCMN.1993.0410512 Published online by Cambridge University Press

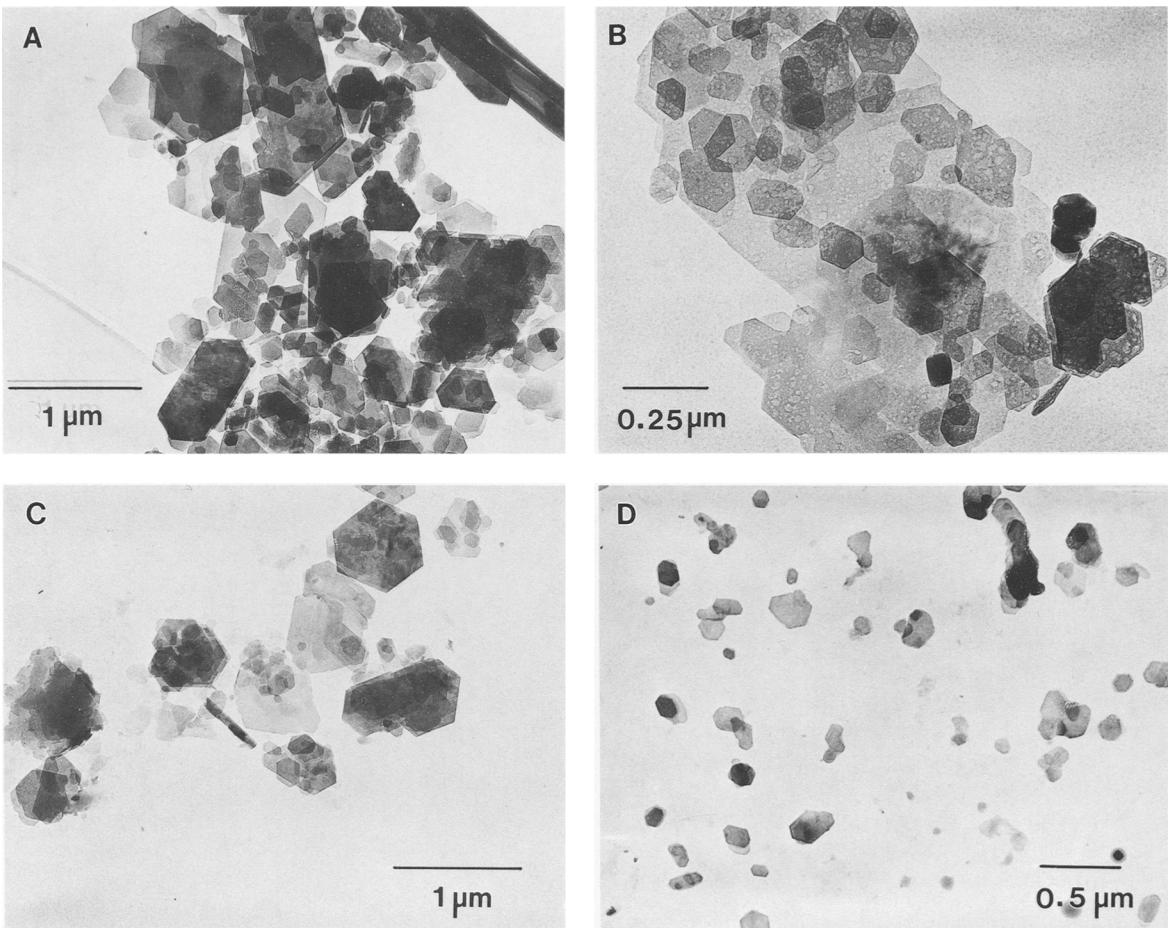


Figure 2. Transmission electron micrographs of dispersed particles from four different size ranges of Weipa kaolinite: A) the bulk sample, without size fractionation; B) size fraction A, nominally >2 μm size, showing both large particles and adhering small particles; C) size fraction C, between 0.5 and 0.6 μm; and D) size fraction E, between 0.3 and 0.4 μm. In the latter two cases, relatively uniform particle sizes can be observed.

(fraction "A") for the Weipa kaolinite. Even though large kaolinite particles are well-dispersed on the substrate, there is clearly a residual amount of finer grained material adhering to the larger particles. This adhesion of smaller particles on larger kaolinite plates appeared to be insignificant for the smaller size fractions. Retention of these smaller, residual particles on larger plates clearly makes difficult the precise estimate of clay particle size distributions using electron microscopy and/or image processing techniques. In addition, the range of particle sizes in the >2 μm fraction is considerably greater than in any other separated fraction. Thus, a large error in the determination of average particle size using measurements from electron micrographs can be expected for the A size fraction. For comparison, Figures 2C and 2D show TEM micrographs of the Weipa C and E size fractions, respectively. Both these fractions show a relatively uniform distribution of particle sizes.

Gravimetric method

Table 1 gives a summary list of weight percentages of the bulk sample determined by gravimetric methods for each of five size fractions separated by centrifugation. The two Georgia kaolinites (averaged data from two sets of analyses) show distinctly different distributions of particles in each size fraction range. In some cases, (e.g., fractions C and D of KGa-2) the same weight percentage value for the given size fraction was obtained for each replicate analysis.

Laser diffraction method

Calibration and reproducibility. For typical clay sizes, it is appropriate to test for both the absolute calibration of the instrument and the reproducibility of results over a given period of time. In this study, a monomodal distribution of latex spheres has been analyzed using laser diffraction with the Malvern Mastersizer E and

https://doi.org/10.1346/CCMN.1993.0410512 Published online by Cambridge University Press

Table 1. Weight percentage* of size fractions.

Fraction	Georgia KGa-1	Georgia KGa-2
A	49 (4)	9 (1)
B	28 (5)	17 (1)
C	13 (4)	23 (0)
D	5 (1)	10 (0)
E	6 (1)	42 (1)

* Values in parentheses are one esd (estimated standard deviation) for replicate analyses.

using image analysis of calibrated SEM images. Figure 3 shows the results of size distribution analyses for this sample of latex spheres via both methods. In Figure 3A, the sizes determined by laser diffraction follow a typical monodisperse distribution with an equivalent spherical particle diameter of 0.33(7) μm. Using the image analysis technique on 1644 individual latex spheres, the average particle diameter for the distribution shown in Figure 3B is 0.34(7) μm. For comparison, Figure 3C shows the same particle size distribution as in Figure 4A using Mie scattering theory as well as for the Fraunhofer diffraction model plotted as volume distribution.

The Malvern Mastersizer E has been carefully configured to provide reproducible results over the 0.1–80 μm size range. In order to test for long-term reproducibility of this technique over periods of weeks and to assess systematic errors not related to shape for a typical clay sample, kaolin-microwhite supplied by Commercial Minerals was used for a series of 70 separate size distribution determinations using the same conditions for the 0.1–80 μm range lens (45 mm). The 70 determinations consisted of seven separate samples of the same material, analyzed 10 times. The reproducibility of results using this technique for the three primary modal values used in this study are given in Table 2. For the size range containing the majority of particles, d_{50}, the coefficient of variance is less than 0.5%. For the lower abundance size ranges, the coefficient of variance ranged between 1% and 2%.

For all size separated fractions of the Georgia samples, replicate analyses were performed on the same size fraction using the Malvern Mastersizer E. In some cases, samples were constantly stirred and ultrasonicated in solution and constantly monitored for size distribution(s) until a unimodal distribution was achieved. This precaution was taken because, for some of the smaller size fractions, agglomeration of particles was observed on initial dispersion in the flow-through cell. Figure 4 shows particle size distributions for two size-separated fractions, Weipa E and Georgia KGa-1 B, taken at various times after initial dispersion in the flow-through cell. For the Georgia sample (Figure 4B), the same size distribution is shown in three measurements taken over a 30-minute period, with the same d_{50} value for each measurement. However, the Weipa

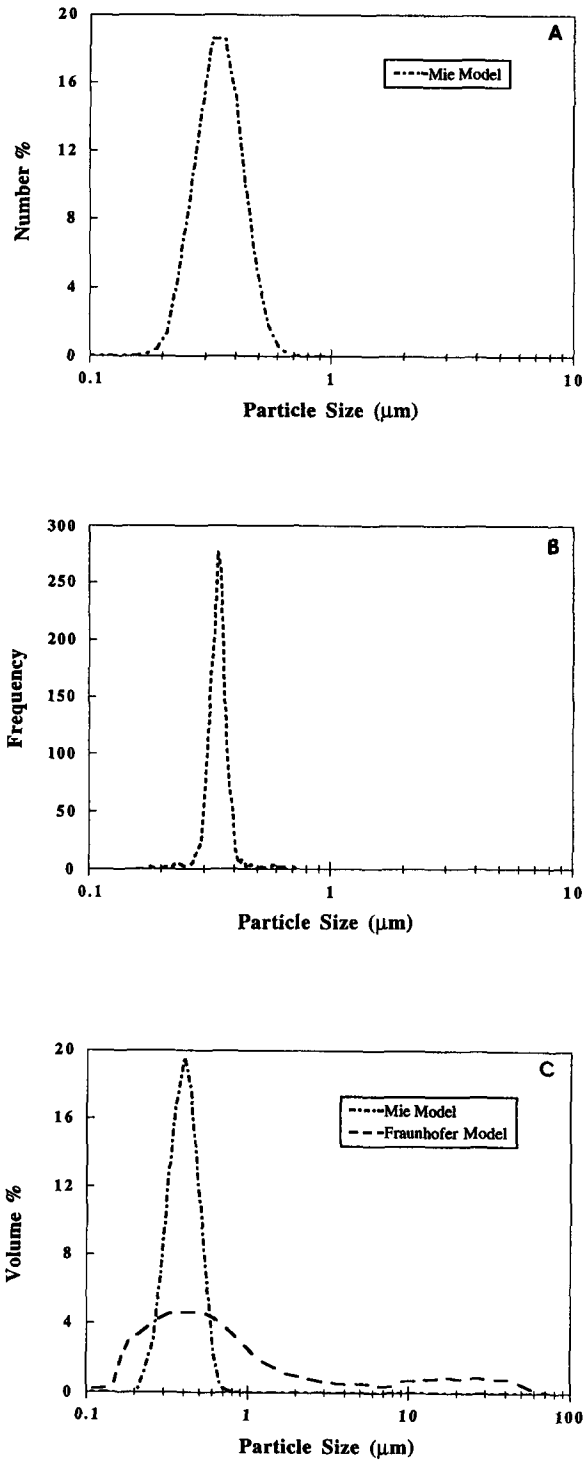
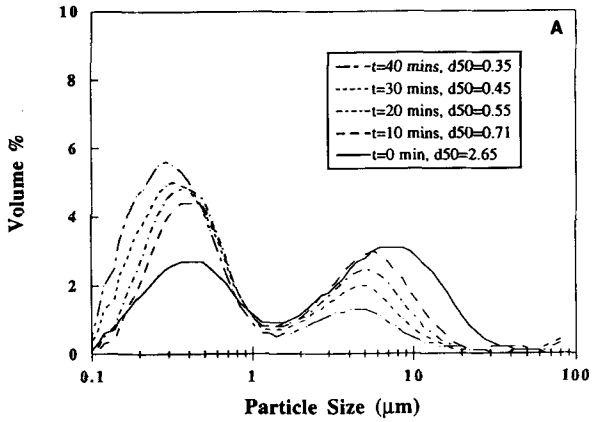


Figure 3. Particle size distributions for a standard sample of latex spheres determined by A) laser scattering using the Mie model and B) image analysis from calibrated electron micrographs. C) indicates distributions from the same laser-scattering data calculated using the Mie and Fraunhofer models respectively.

https://doi.org/10.1346/CCMN.1993.0410512 Published online by Cambridge University Press



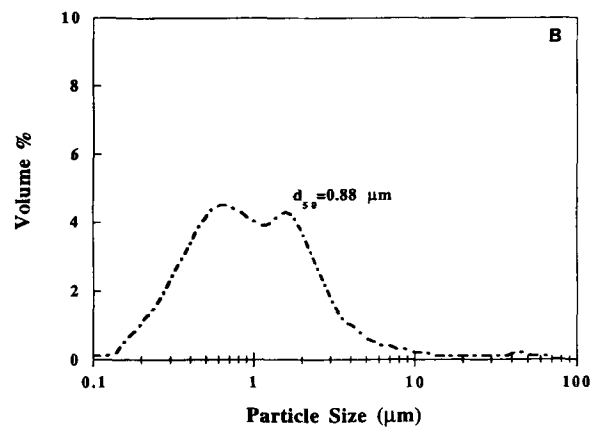
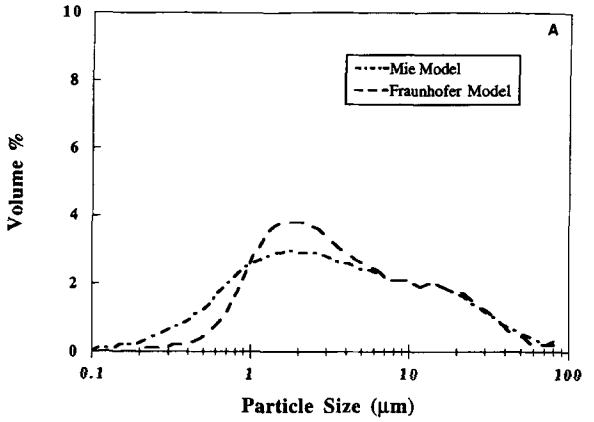


Figure 4. Particle size distributions determined by laser scattering for A) Weipa E size fraction, between 0.3 and 0.4 μm; and for B) Georgia KGa-1 B fraction, between 0.6 and 2.0 μm. For the Weipa E sample, the size distribution changed with time (t = 0 min to t = 40 min) due to particle agglomeration in solution. After 40 min stirring and dispersion, this sample showed a consistent near-unimodal size distribution. In contrast, Georgia KGa-1 size fraction B showed no variation of size distribution with time.



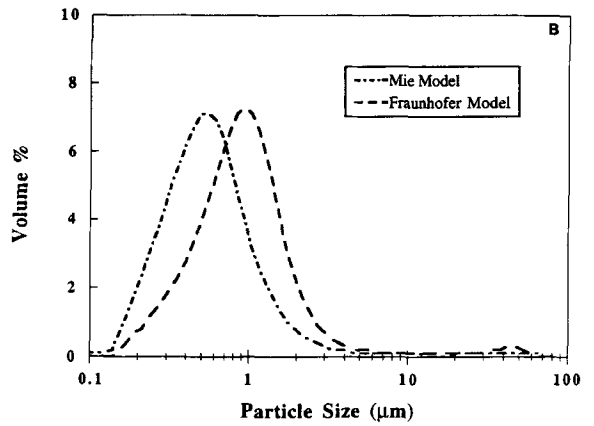


Figure 5. Comparison of particle size distributions for A) a bulk sample of Georgia kaolinite KGa-1 and B) size fraction C, between 0.5 and 0.6 μm of KGa-1. In each graph, size distributions are calculated by the Mie and Fraunhofer models from the same scattering data.

E fraction displays characteristics during particle sizing using laser scattering that are consistent with high levels of particle agglomeration. This fraction initially shows a bimodal size distribution (each of approximately equal intensity), but with time and continued stirring of particles in the presence of the dispersant Calgon, this bimodal distribution transforms to a predominantly unimodal distribution. No further change in the size distribution was observed in any of these smaller size fractions with time once the predominantly unimodal distribution was achieved. All data for small size fractions presented in this study are determined from samples that have been dispersed as well as possible for periods of up to 30 minutes using the same method.

Kaolinite fractions. Table 3 lists the averaged particle diameters for replicate analyses of two different 5g samples of KGa-1 and KGa-2, which were size-separated by the method of Tanner and Jackson (1947) and determined by laser scattering. Data compiled under the heading "Average" are the average of all four sets of replicate analyses from both KGa-1 and KGa-2, along with calculated standard deviations for each particle diameter. In order to obtain an accurate assessment of the size range of the majority of particles in each separated fraction, the d_{70} and d_{30} values for each fraction are listed in Table 3 along with the d_{50} value. For monodisperse samples, d_{70} and d_{30} provide an estimate of sizes for the majority of particles in the fraction (>50% by volume), provided the size distribution curve is not a straight line. While data in Table 3 show that there is clearly overlap in the sizes of particles separated into different fractions, graphs of these laser-scattering data indicate that the relative proportion of particles that overlap into adjacent size "bins" is generally less

https://doi.org/10.1346/CCMN.1993.0410512 Published online by Cambridge University Press

Table 2. Reproducibility test for Malvern Mastersizer E using clay particles (n = 70).

	d_{90}	d_{50}	d_{10}
Mean (μm)	11.75	2.84	0.633
Standard deviation (μm)	0.119	0.013	0.011
Coefficient variance (%)	1.01	0.47	1.70

than the predominant size fraction. Thus, fraction B of KGa-1 contains some particles that are <0.6 μm diameter (the lower cut-off for fraction B; see below), but the proportion of particles <0.6 μm diameter is significantly less than that in fraction C. These general relationships are also evident from a detailed inspection of the size distribution data plotted for individual size fractions of KGa-1 and KGa-2 (not shown). Some degree of overlap between these size ranges could presumably be reduced by successive (or additional) centrifugations of the respective size fractions.

Estimates of the approximate size ranges for each successive fraction, as measured by laser scattering, are given in Table 4 and are compared with the ranges predicted from the Tanner and Jackson (1947) nomogram. The size ranges from laser scattering are obtained by taking the mean upper and lower values of each adjacent size bin and rounding to the nearest whole number. For example using Table 3, the value for the upper range of fraction "B" (and the lower range of fraction "A") is determined by:

$$B_{upper} = (d_{30} + d_{70})/2 = (2.32 + 1.44)/2 = 1.88;$$
$$\text{rounding up } B_{upper} = 2.0\ \mu m.$$

For the upper range of fraction D, the estimate is obtained by the calculation (0.38 + 0.57)/2 = 0.48 using values from Table 3. After rounding up this number, the upper size range for fraction D is 0.5 μm. A similar approach for an estimate of the size range determined by laser scattering has been used for each of the six size fractions. These estimates are given in Table 4 and are based upon the averaged data for KGa-1 and KGa-2 samples listed in Table 3.

Scattering algorithms. Size distribution plots for two different types of samples, each calculated with different algorithms are given in Figure 5. In Figure 5A, distributions for the bulk sample of KGa-1 are shown. Figure 5B shows a size distribution for fraction C (i.e., 0.5–0.6 μm) of the Georgia KGa-1 sample. In both figures, the Fraunhofer and Mie models for the reduction of experimental scattering data to size distribution are presented.

DISCUSSION

Laser scattering techniques primarily rely on the angular distribution of forward scattered light to infer the size distribution(s) of particles suspended in solution.

Table 3. Size data for Georgia kaolinites.

Sample	Fraction	d_{70}	d_{50}	d_{30}
KGa-1	A	8.74 (106)	4.60 (16)	2.47 (3)
	B	1.60 (17)	0.97 (13)	0.58 (5)
	C	0.73 (5)	0.53 (2)	0.38 (1)
	D	0.58 (8)	0.41 (1)	0.31 (1)
	E	0.48 (1)	0.35 (0)	0.26 (0)
KGa-2	A	5.83 (77)	3.64 (33)	2.16 (17)
	B	1.28 (13)	0.73 (8)	0.47 (4)
	C	0.74 (1)	0.53 (4)	0.38 (2)
	D	0.56 (5)	0.42 (4)	0.31 (2)
	E	0.49 (2)	0.36 (2)	0.27 (1)
Average	A	7.28 (185)	4.12 (60)	2.32 (20)
	B	1.44 (23)	0.85 (17)	0.52 (7)
	C	0.73 (5)	0.53 (2)	0.38 (2)
	D	0.57 (6)	0.41 (2)	0.31 (1)
	E	0.49 (1)	0.35 (1)	0.27 (1)

Values in μm; esds in parentheses.

The effectiveness of this approach depends to a large extent upon the sophistication of models used to predict the scattering of light from individual particles with an assumed shape and optical properties (e.g., absorption, refractive index). In addition, the optical configuration of the sample, lenses, and various photon detectors influences the reliability of the laser scattering technique. A rigorous solution to the scattering of light by a particle with dimensions similar to, or greater than, the incident wavelength was given by Mie (1908). In Mie's model, exact solutions for scattering by a homogeneous, partially absorbing sphere can be calculated and are now feasible for laboratory instrumentation due to the development of powerful personal computers and microprocessors. The use of Mie theory for prediction of scattering from particles in the smaller size fractions (i.e., <5 μm diameter) is clearly an invaluable development for clay-size samples (McCave *et al.*, 1986). Ideally, algorithms for both Fraunhofer and Mie models (Pugh, 1987), as well as for the condition of anomalous scattering, should be available in laser scattering particle sizers for materials <5 μm in equivalent diameter (Miller and Lines, 1988). These options for calculation of size distributions are increasingly available in modern laser diffraction instruments.

The laser-scattering technique should not be con-

Table 4. Estimated size ranges for separated fractions.

Fraction	Tanner and Jackson (1947)	Laser scattering
A	>2.0	>2.0
B	1.0–2.0	0.6–2.0
C	0.5–1.0	0.5–0.6
D	0.4–0.5	0.4–0.5
E	0.3–0.4	0.3–0.4
F	<0.3	<0.3

Values in μm.

https://doi.org/10.1346/CCMN.1993.0410512 Published online by Cambridge University Press

fused with photon correlation spectroscopy (PCS), which utilizes a laser beam to illuminate a dilute suspension of particles in a liquid while changes in light intensity are measured as the particles move under Brownian motion (Miller and Lines, 1988). PCS is also known as autocorrelation spectroscopy, quasi-elastic light scattering, intensity fluctuation spectroscopy and dynamic light scattering (Miller and Lines, 1988). With PCS, changes in light intensity as it is scattered from particles moving under Brownian motion are measured. The frequency of Brownian motion of a small particle is inversely proportional to particle size. In general, PCS is designed for the routine analysis of dilute suspensions of particles ranging in size from 40 nm up to about 3 μm (Gahwiller, 1980).

With laser scattering, a diffraction pattern is formed when a (monochromatic) beam of light falls onto a particle. The diffraction of this light is dependent upon, among other parameters, the size of the particle. If a lens is placed in the light path behind the particle(s) and a suitable detector placed at the focal point of the lens, then diffracted light will be imaged concentrically at a distance from the axis, which is a function of the particle diameter. In general, these diffracted light intensities are dependent not only on the particle size but also on the real and imaginary refractive indices of the scatterer (Dodge, 1984). However, by restricting the scattering measurements to small angles in the forward diffraction direction, and if the diameters of the scatterers are much larger than the wavelength of the radiation, particle properties are unimportant for solution of the size dependence of diffracted light intensity. Furthermore, dilute solutions of particle suspensions are not a requirement for this technique. As noted above, if light scattering from particles of size similar to the incident wavelength is calculated according to the model of Mie (1908), exact solutions to particle size distributions for particles <2 μm can be obtained (Dodge, 1987).

Laser scattering is a technique suited to quantitative analysis of particle size distribution(s) because, on average, greater than 10^5 particles are measured each time the laser beam illuminates particles within the sample cell (i.e., for each analysis). In addition, the technique is rapid (an analysis may take less than 30 min) and does not require very large amounts of sample. However, there has been limited acceptance of this technique within the clay and soil sciences presumably because of perceived concerns with 1) absolute calibration of these instruments and 2) documented examples of poor results for clay size distributions when compared with conventional sedimentation techniques (e.g., McCave *et al.,* 1986).

Calibration and reproducibility. Calibration of laser diffraction spectrometers has been the subject of considerable study by the powder technology community (Dodge, 1984, 1987; Tuzun and Farhadpour, 1985; de Boer *et al.,* 1987) and had generally been considered a difficult problem once an instrument left the manufacturer (Dodge, 1984). In the past, it had been assumed that laser diffraction instruments did not require calibration once constructed, because of the presumed linearity of the light detection system over three orders of magnitude as a function of angle from the optical centerline. However, theory and experiment did not always provide good agreement for a range of datasets (Dodge, 1984; McCave *et al.,* 1986), particularly in the case of Fraunhofer diffraction or anomalous dispersion calculations of the diffraction phenomena. For this case, laboratory-based calibration procedures for Malvern instruments were developed (Dodge, 1984) and have been used to carry out interlaboratory comparisons of drop-sizing instruments (Dodge, 1987). In general, laser diffraction instruments provided good to excellent agreement between laboratories (Dodge, 1987). A fundamental study on the principles of laser diffraction spectrometry by de Boer *et al.* (1987), established that particle sizes calculated on Mie-scattering theory provided excellent results on samples that had been previously calibrated by independent methods. In addition, results were similarly predictable for the lower size ranges and for cases in which the refractive indices of the disperse and continuous phases are similar. This approach by de Boer *et al.* (1987) showed that it is possible to predict particle size distributions via the Mie-scattering theory without calibrating an instrument using standard materials.

Results from the independent sizing measurements in this study using laser scattering and image analysis also confirm these earlier conclusions that laser diffraction, using Mie theory for data reduction, provides an excellent estimate of particle size. As shown in Figure 3, results from these two techniques for monodisperse, spherical particles show excellent agreement in a size range <2 μm. While this experiment does not explicitly reproduce the same shape characteristics of a typical clay particle assemblage, the absolute calibration of size using laser scattering is well within the estimated standard deviations using well calibrated image analysis techniques. Statistically, these results show that the average values from each technique are equivalent at the 0.01% level using a Student's t-test for two independent samples.

Similarly, this result can be achieved in a reproducible fashion. The data presented in Table 2 show that modal values for particle size (d_{50} values) can be determined with a relative precision of $<1\%$. Furthermore, values for the extreme tails of a size distribution (i.e., d_{90} and d_{10}) can be reproduced with a relative precision of $<2\%$. Values for intermediate average particle diameters, such as d_{70} and d_{30}, which are used in Table 3, are assumed to have a relative precision between the lower and upper limits of this reproducibility

https://doi.org/10.1346/CCMN.1993.0410512 Published online by Cambridge University Press

test (i.e., between 1% and 2%). These general estimates of reproducibility of the laser scattering technique are supported by the replicate sizing results for samples KGa-1 and KGa-2 given in Table 3. Thus, the reproducibility of this technique for clay-shaped particles over the 0.1 μm to 80 μm size range is extremely high compared with that measured, for example, by McCave *et al.* (1986), who used anomalous dispersion algorithms for the reduction of diffraction intensities to particle size distribution. Comparisons of these average particle size data shown in Table 3 using Mie model calculations in the <1.0 μm size range are excellent.

Size fractionation. Using the laser scattering method for size distribution determination, the average d_{50} values for all size fractions of samples KGa-1 and KGa-2 generally fall within the range predicted by the method of Tanner and Jackson (1947). Indeed, size distribution values for each fraction show that the procedure developed by Tanner and Jackson (1947) is effective in separating particles into narrow size ranges below 2 μm with predominant, or modal, sizes that progressively decrease. The lower size limit for fraction B is different using the laser-scattering method compared with that estimated from the nomogram of Tanner and Jackson (1947). This difference (a value of 0.6 μm compared with 1.0 μm) is not readily explicable, but may be related to the adherence of smaller-sized particles to the larger (i.e., ~1.0 μm) particles in fraction B. Presumably, factors such as surface charge or minor variations in composition may influence the degree of adherence of small particles to larger particles. Furthermore, smaller particles may be less prone to adherence of different sized particles during the fractionation procedure and may also show hydrodynamic properties more akin to spherical-shaped particles in fluid flow. Thus, the difference in size ranges estimated by Tanner and Jackson (1947) and determined by laser scattering is reduced considerably for fractions D, E, and F. There is a range of particle sizes within each separated fraction, which, in some cases, overlaps with the adjoining fractions. This separation into progressively smaller size ranges, but with overlapping values in the "tails" of the size distributions for each fraction, appears to be consistent for each kaolinite studied and for replicate analyses.

For modal analyses of size distribution data (i.e., d_{50} values), the average values for each size separated fraction are remarkably similar for both KGa-1 and KGa-2 and, thus, the average values for four replicate analyses show correspondingly small standard deviations in the "Average" columns. The maximum coefficient of variance for the smaller size fractions (i.e., C, D, and E) is ~5%, while the larger size fractions show high coefficients of variance at ~14%. A coefficient of variance of ~5% for four analyses compares favorably with a ~1% coefficient of variance for a sample set of seventy analyses (Table 2). The coefficient of variation for the larger size fractions, particularly fraction A, is not unexpected due to the considerable range in particle sizes >2 μm for both samples. The relative errors for determination of large particle sizes for KGa-2 are lower than for KGa-1 because there is a lower proportion of large particles in KGa-2 and the range of sizes is smaller (see Table 1). However, for size fractions <2 μm, the values for the different fractions are clearly reproducible for either KGa-1 or KGa-2. These summary data support the suggestion that the method of separation by Tanner and Jackson (1947) provides size fractions that consistently show d_{50} modal values that lie within specific estimated size ranges. These size ranges, while approximate, are determined by laser-scattering techniques with a high level of reliability and, for a given experimental configuration, appear to be internally consistent.

Scattering models. As shown in Figures 3C and 5, the Fraunhofer diffraction model shows sharp discontinuities or markedly different distributions for particle sizes less than ~2 μm for monodisperse latex spheres and the Georgia KGa-1 bulk sample, respectively. These results for the Fraunhofer model are in contrast to electron microscopy observations and calculated weight percentage values for separated fractions <2 μm in size. For example, the equivalent spherical diameter for latex spheres modeled using Mie theory is 0.33(7) μm, while the span for this distribution is 0.54. The span for a sample distribution is given by the relation $(d_{90}-d_{10})/d_{50}$ and is a measure of the spread of particle sizes in a given distribution. A low value for the span (i.e., <1.0) indicates a very narrow size distribution for a particular sample. For the Fraunhofer model, the calculated particle sizes are very broad (span ~24.78) and thus, an estimate of equivalent spherical diameter assuming a monomodal distribution is precluded. An alternative estimate of particle diameter may be obtained from the d_{50} value, which, for this model, is 0.55 μm. This latter value, and in particular, the graph of size distribution using a Fraunhofer model shown in Figure 3C, is considerably at variance with that determined by image analysis techniques as well as that modeled by Mie scattering.

For the bulk KGa-1 sample, there is also considerable divergence of the size distribution graphs for the Mie model and the Fraunhofer model at sizes <2 μm (Figure 5A). In Figure 5A, the Fraunhofer model shows a pronounced mode at about 2 μm. The appearance of modes with constant position is also noted by McCave *et al.* (1986) in their study of natural sediments using laser-scattering techniques. McCave *et al.* (1986) suggested that these modes appear because of the inability of the inversion scheme (i.e., the model for light scattering) to cope with the level of noise produced by light

https://doi.org/10.1346/CCMN.1993.0410512 Published online by Cambridge University Press

scattered from clays in the <2 μm size range. There is good agreement between the Fraunhofer and Mie models for sizes above about 7 μm. The Mie model shows a gradual decrease in the proportion of particles in the <2 μm range. This distribution is consistent with the weight percentage values for each size fraction determined by independent gravimetric methods as shown in Table 1.

The effect of an inappropriate scattering model, such as the Fraunhofer model, on the calculated size distribution of a size fractionated sample in the <2 μm range is demonstrated in Figure 5B. In this figure, both the Mie and the Fraunhofer model distributions for KGa-1 fraction "C" (i.e., 0.5 μm–0.6 μm) are shown. For the Fraunhofer model, the size distribution is shifted to higher values. The d_{50} values for each scattering model are 0.51 μm and 0.83 μm, for the Mie and Fraunhofer models, respectively. In addition, the Fraunhofer model shows a small, but significant mode at very high particle sizes (e.g., 30 μm–60 μm). The presence of such large particles in this size-fractionated sample could not be confirmed by any imaging or other independent technique. It is clear that this mode is an artifact of the size distribution calculation using the Fraunhofer model (McCave *et al.,* 1986).

CONCLUSIONS

An assessment of laser-scattering techniques for particle size determination of clays indicates that the method provides a rapid and reliable approach to size analyses if suitable models for light scattering are incorporated into data analysis. In particular, for particle sizes less than a few micrometers, it is essential to utilize Mie theory for exact calculation of light scattering by particles that approach the size of the incident light wavelength. Using Georgia kaolinite Source Clays as test samples, six size fractions were prepared for replicate analyses using the separation methods outlined by Tanner and Jackson (1947). Comparison of particle sizes determined by laser scattering and calculated from nomograms (Tanner and Jackson, 1947) indicates that, in general, there is good agreement between the size range estimates for both methods. The high reliability of the laser-scattering technique when Mie theory is applied to scattering intensities suggests that the size ranges determined for the separated fractions should hold for all types of kaolinites provided the method outlined by Tanner and Jackson (1947) is followed.

ACKNOWLEDGMENTS

This work benefited from discussions with Roger Taylor from Scientific Adaptations and John Thompson, Research School of Chemistry, Australian National University. In addition, comments from Ray Ferrell on an earlier version of this manuscript are greatly appreciated. Funding for this work was provided by the Australian Research Council through Grants A290891 (to IDRM) and AB9130015 (to IDRM and J. Thompson).

REFERENCES

Allen, T. (1981) *Particle Size Measurement:* 3rd ed., Powder Technology Series, Chapman and Hall, London, 678 pp.

Bayvel, L. P. and Jones, A. R. (1981) *Electromagnetic Scattering and its Applications:* Applied Science, London, 289 pp.

Brindley, G. W., Kao, C.-C., Harrison, J. L., Lipsicas, M., and Raythatha, R. (1986) Relation between structural disorder and other characteristics of kaolinites and dickites: *Clays & Clay Minerals* **34,** 239–249.

Brown, D. J. and Felton, P. G. (1985) Direct measurement of concentration and size for particles of different shapes using laser light diffraction: *Chem. Eng. Res. Des.* **63,** 125–134.

Cooper, L. R., Haverland, R. L., Hendricks, D. M., and Knisel, W. G. (1984) Microtrac particle-size analyzer: An alternative particle-size determination method for sediment and soils: *Soil Science* **138,** 138–146.

Cornillault, J. (1972) Particle size analyser: *Applied Optics* **11,** 265–268.

De Boer, G. B. J., de Weerd, C., Thoenes, D., and Goossens, H. W. J. (1987) Laser diffraction spectrometry: Fraunhofer diffraction versus Mie scattering: *Part. Charact.* **4,** 14–19.

Dodge, L. G. (1984) Calibration of the Malvern particle sizer: *App. Optics* **23,** 2415–2419.

Dodge, L. G. (1987) Comparison of the performance of drop-sizing instruments: *App. Optics* **26,** 1328–1341.

Fripiat, J. J. and van Olphen, H., eds. (1979) *Data Handbook for Clay Materials and other Non-metallic Minerals:* Pergamon Press, New York, 346 pp.

Gahwiller, C. (1980) A new method for the rapid determination of the averaged size and an index of polydispersity of submicron particles in liquids using laser light-scattering spectroscopy: *Powder Technology* **25,** 11–13.

Hassanipak, A. A. and Eslinger, E. (1985) Mineralogy, crystallinity, O^{18}/O^{16}, and D/H of Georgia kaolins: *Clays & Clay Minerals* **33,** 99–106.

Hinckley, D. N. (1963) Variability in "crystallinity" values among the kaolin deposits of the coastal plain of Georgia and South Georgia: *Clays & Clay Minerals* **11,** 229–235.

Lombardi, G., Russell, J. D., and Keller, W. D. (1987) Compositional and structural variations in the size fractions of a sedimentary and hydrothermal kaolin: *Clays & Clay Minerals* **35,** 321–335.

McCave, I. N., Bryant, R. J., Cook, H. F., and Coughanowr, C. A. (1986) Evaluation of a laser-diffraction-size analyzer for use with natural sediments: *J. Sed. Petrol.* **56,** 561–564.

Mie, G. (1908) Beitrage zur Optik truber Medien, speziell kolloidaler Metallosungen: *Ann. Physik* **25,** 377.

Miller, B. V. and Lines, R. W. (1988) Recent advances in particle size measurements: A critical review: *CRC Critical Reviews in Analytical Chemistry* **20,** 75–116.

Murray, H. H. and Lyons, S. C. (1956) Correlation of paper-coating quality with degree of crystal perfection of kaolinite: *Clays & Clay Minerals* **4,** 31–40.

Olivier, J. P. and Sennett, P. (1973) Particle size-shape relationships in Georgia sedimentary kaolins. II: *Clays & Clay Minerals* **21,** 403–412.

Plancon, A. and Zacherie, C. (1990) An expert system for

https://doi.org/10.1346/CCMN.1993.0410512 Published online by Cambridge University Press

the structural characterization of kaolinites: *Clay Miner.* **25,** 249–260.

Pugh, D. G. (1987) Analysis of materials in the 0.12–300 micron range (using Mie and Fraunhofer theories): *Curr. Aware. Part. Technol.* **20,** 243–251.

Tanner, C. B. and Jackson, M. L. (1947) Nomographs of sedimentation times for soil particles under gravity or centrifugal acceleration: *Soil Sci. Soc. Amer. Proc.* **11,** 60–65.

Tettenhorst, R. T. and Corbato, C. E. (1986) Properties of a sized and ground kaolinite: *Clay Miner.* **21,** 971–976.

Tuzun, U. and Farhadpour, F. A. (1985) Comparison of light scattering with other techniques for particle size measurement: *Part. Charact.* **2,** 104–112.

(Received 4 September 1992; accepted 11 June 1993; Ms. 2273)

https://doi.org/10.1346/CCMN.1993.0410512 Published online by Cambridge University Press